

Determining TG-43 brachytherapy dosimetry parameters and dose distribution for a ^{131}Cs source model CS-1

M. Yazdani and A.A. Mowlavi*

Department of Physics, Tarbiat Moallem University of Sabzevar, Sabzevar, Iran

Background: Monte Carlo determination of TG-43 brachytherapy dosimetry parameters and dose distribution calculation for ^{131}Cs source model CS-1 are presented in this study. **Materials and Methods:** The dose distribution was calculated around the ^{131}Cs Model CS-1 located in the center of 30 cm \times 30 cm \times 30 cm water, and soft tissue phantoms cube using MCNP code by Monte Carlo method. The percentage depth dose (PDD) variation along the different axis, parallel and perpendicular, the source was calculated. Then, the isodose curves for 100%, 75%, 50% and 25% PDD were constructed. Finally, $F(r, \theta)$ and $g(r)$ dosimetry parameters of TG-43 protocol have been determined. **Results:** Results obtained show that the Monte Carlo method could only calculate dose deposition in high gradient region, near the source, accurately. The energy cut off was found to be 1 eV and the error in the calculations was less than 2%. **Conclusion:** The isodose curves of the CS-1 ^{131}Cs source were constructed from dose calculation by MCNP code. The calculated dosimetry parameters for the source were in agreement with previously published results. Iran. J. Radiat. Res., 2007; 5 (2): 85-90

Keywords: ^{131}Cs source, dose distribution, isodose curves, MCNP code.

INTRODUCTION

Theoretical and experimental dosimetric studies have been supplied useful information on the dependence of the brachytherapy source geometry and materials (1-5). Usually, Monte Carlo method is used to define dose distribution function, the radial dose variation, and the dose calculation close to the source in brachytherapy. Chen *et al.* (6). calculated the distribution of absorbed dose around commercially available ^{131}Cs seeds model Cs-1 by Monte Carlo simulation.

^{131}Cs has a higher average energy than any other commonly used prostate brachytherapy isotope in the market such as ^{103}Pd and ^{125}I . Energy is a key factor in how uniformly the radiation dose can be delivered throughout

the prostate. Also, ^{131}Cs has the shortest half-life of any prostate brachytherapy isotope at 9.7 days. ^{131}Cs delivers 90% of the prescribed dose to the prostate in just 33 days compared to 58 days for ^{103}Pd and 204 days for ^{125}I . The short half-life of ^{131}Cs reduces the duration of time during which the prostate receives the irritating effects of the radiation. Another benefit to the short half-life of ^{131}Cs is what is known as the biological effective dose (BED). BED is a way for providers to predict how an isotope will perform against slow versus fast growing tumors. Studies have shown ^{131}Cs is able to deliver a higher BED across a wide range of tumor types than either ^{125}I or ^{103}Pd . Although prostate cancer is typically viewed as a slow growing cancer it can present with aggressive features. ^{131}Cs 's higher BED may be particularly beneficial in such situations. Currently, the IsoRay ^{131}Cs seed is used exclusively for the treatment of prostate cancer (7-12). For calculating dose distribution and TG-43 brachytherapy parameters usually Monte Carlo codes as MCNP, EGS4, GEANT4 are applied. In this present work, we have used MCNP4C code (12) to calculate relative dose in the phantom.

MATERIALS AND METHODS

^{131}Cs source

The ^{131}Cs seed was developed after invention by Lawrence and a ^{131}Cs (model Cs-1) received 510(k) FDA clearance in 2003 (11). New low-energy interstitial brachytherapy seeds containing ^{131}Cs source model Cs-1 were

*Corresponding author:

Dr. Ali Asghar Mowlavi,

Department of Physics, Tarbiat Moallem University of Sabzevar, P.O. Box 397, Sabzevar, Iran.

Fax: +98 571 4411161

E-mail: amowlavi@sttu.ac.ir

introduced by IsoRay Medical Inc. The ^{131}Cs with a half life of 9.7 days emits γ -ray with highest peaks from 29 to 34 keV ⁽³⁾. Offsetting, with the disadvantage of its high specific activity, translated into the possibility of developing physically small, high-activity sources as a replacement for ^{192}Ir in brachytherapy ⁽¹⁰⁾.

Figure 1 shows a schematic cross-sectional view of the IsoRay ^{131}Cs brachytherapy seed (Model CS-1). The titanium tube has an outer diameter of 0.8 mm with a wall thickness of 0.05 mm, thus an inner diameter of 0.7 mm. The center X-ray marker is a 0.25 mm diameter gold wire. The wire is surrounded by a glass and ceramic tube with nominal dimensions of 0.4 mm inside diameter and 0.65 mm outside diameter. The overall lengths of the seeds tested were 4.7 mm, based on a 4.5-mm long tube with 0.1 mm thick caps on each end. The core length was 4.2 mm to allow clearance inside the tube for fit-up and welding ^(2, 3). We assumed the radioactive material to be uniformly distributed within the ^{131}Cs active core. The photons spectrum emitted per decay of ^{131}Cs and their intensity are shown in table 1 ⁽³⁾.

Method of dose calculation in water and soft tissue phantoms

The Monte Carlo N-Particle code (MCNP version 4C) with photon cross-section library DLC-200 was used for the dose rate simulations ⁽¹²⁾. The cutoff energy was set at 1.0 keV. In the present work, the dose distribution has been calculated around the ^{131}Cs source, located in the center of 30cm \times 30cm \times 30 cm phantom as shown in figure 2 by using tally F6:p of MCNP code ⁽¹²⁾. The tally in the sphere of 0.1 mm diameter cell was evaluated as dose in the point center of

Table 1. The photon spectrum of ^{131}Cs source is used in our simulation.

Energy (keV)	Radiation Source	Intensity
16.6	Fluorescent (Nb - K_{α})	0.007 ± 0.0003
18.7	Fluorescent (Nb - K_{β})	0.001 ± 0.00006
29.7	^{131}Cs - K_{α}	1.000
33.6	^{131}Cs - $K_{\beta 1, \beta 3}$	0.201 ± 0.0007
34.4	^{131}Cs - $K_{\beta 2}$	0.050 ± 0.0003

the sphere. First, along the X axis with 0.1 mm step and along the Y axis with 0.1 mm step, and the relative dose curves were calculated. The dose distribution was normalized to 100% at the point X=2 mm, Y=0 mm, arbitrary. Isodose points were found from relative dose curves by interpolate method. Soft tissue composition used in this study, are listed in table 2 ⁽¹⁵⁾. Mass density for soft tissue was 1.04 g/cm³.

TG-43 formalism

Radial dose function and anisotropy function are dosimetry important parameters that must be determined according to TG-43 protocol, further to the comparison of our result with those obtained by others. According to the published protocol ^(4, 14), $\dot{D}(r, \theta)$ the absorbed dose rate, $F(r, \theta)$ is the anisotropy function, $g(r)$ is radial dose function are expressed as:

$$\dot{D}(r, \theta) = S_k \Lambda \frac{G(r, \theta)}{G(r_0, \theta_0)} g(r) F(r, \theta) \quad (1)$$

$$F(r, \theta) = \frac{\dot{D}(r, \theta)}{\dot{D}(r_0, \theta_0)} \frac{G(r_0, \theta_0)}{G(r, \theta)} \quad (2)$$

$$g(r) = \frac{\dot{D}(r, \theta_0)}{\dot{D}(r_0, \theta_0)} \frac{G(r_0, \theta_0)}{G(r, \theta_0)} \quad (3)$$

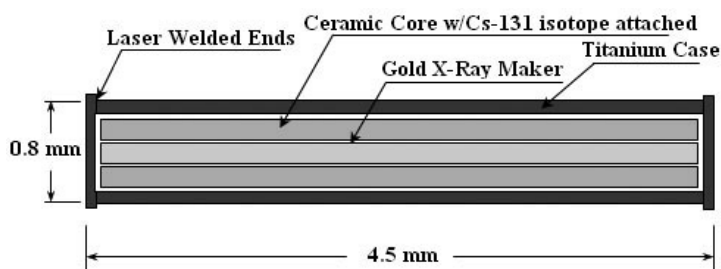


Figure 1. Schematic diagram of the CS-1 ^{131}Cs source structure

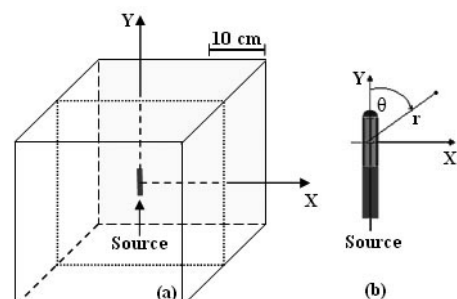


Figure 2. a) Scheme of water/soft tissue phantom which ^{131}Cs source is located in the centre of cube, b) the source in large size.

Table 2. Soft tissue composition and mass density for soft tissue used in MCNP input ⁽⁴⁵⁾.

Element	Weight Fraction	Element	Weight Fraction
H	10.454	S	0.204
C	22.663	Cl	0.133
N	2.490	K	0.208
O	63.525	Ca	0.024
Na	0.112	Fe	0.005
Mg	0.013	Zn	0.003
SiO	0.030	Rb	0.001
P	0.134	Zr	0.001

Where S_k is the air kerma strength, Λ is the dose rate constant, $G(r, \theta)$ is the geometry factor, and (r_0, θ_0) is the reference point.

RESULTS

Monte Carlo dose calculation

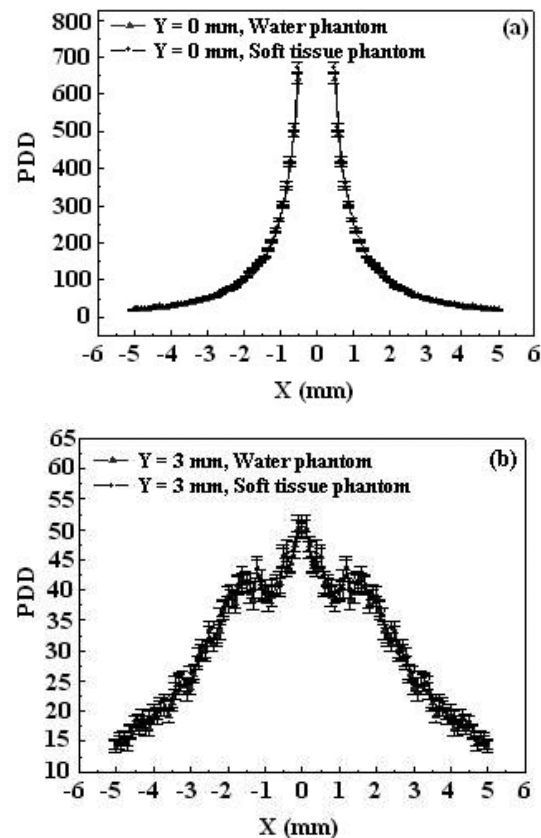
Figure 3 shows the PDD variation along the $Y=0$ mm, and $Y=3$ mm for water and soft tissue medium. It is clear that the PDD has been decreased about 10 times in this short distance; as well as the effect of source shield is obvious in this figure. The PDD variation along the $X=0.5$ mm and $X=2$ mm are shown in figure 4. It can be seen, due to the low energy photons deposit their energy near the source, the PDD fall down about 7 times when going from $X=0.5$ mm to $X=2$ mm, and the PDD curve change from smooth flat shape to a semi-Gaussian shape. The calculated results show a good agreement between water and soft tissue PDD data. The isodose curves for PDD = 100%, 75%, 50% and 25% results in water and soft tissue phantoms are shown at figures 5-a and 5-b. It is well clear that $D = D(r, \theta)$, dose distribution depends to r and θ , distance from the center of source and polar angle, respectively. As seen, the dose is falling in 5 mm from reference point about 4 times. Thus, this seed shouldn't apply in small tumors with size smaller than 5mm.

These results have been used to compute anisotropy function and radial dose function

in next subsection. In our running, the energy cut off was 1eV, the relative error in these calculations is less than 2%, and the time, that is needed for any programs running are about 240 minutes with a computer Pentium 4 Intel CPU 3.06 GHz.

Determination of TG-43 dosimetry parameters

The MCNP calculated results of the anisotropy function, $F(r, \theta)$, against r for the model CS-1 seed at 0° to 80° interval are tabulated in table 3 for water and soft tissue phantoms. Maximum percentage difference of anisotropy function for the phantoms are 2.82%, 3.79%, 4%, 4.71%, 2.31%, 2.53%, 3.49%, 3.80%, 4.67%, 4.72%, 6.17% at $r = 0.5, 0.75, 1, 2, 3, 4, 5, 6$, and 7 cm, respectively. Most of these maximum differences are belong to $\theta=10^\circ$ angle. The results demonstrate it would be more exact if dosimetry parameters of soft tissue phantom for medical application used instate of the

**Figure 3.** PDD variation along (a) $Y=0$ mm and (b) $Y=3$ mm.

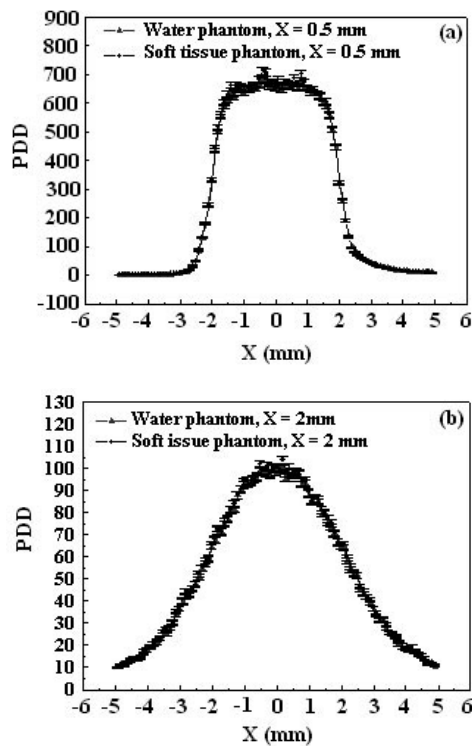


Figure 4. PDD variation along (a) $X=0.5$ mm and (b) $X=2$ mm.

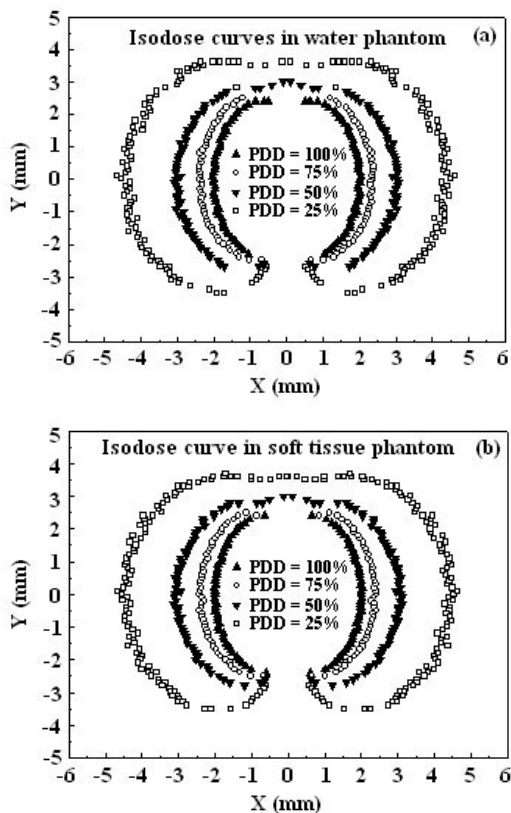


Figure 5. The isodose curves, a) in water phantom, b) in soft tissue phantom (the reference Point: $X=2$ mm, $Y=0$ mm).

water data, although near the source data for both phantoms are very close to each other.

DISCUSSION

Radial dose function and anisotropy function are dosimetry important parameters that have been determined to compare our result with which was obtained by others. Our computational results of $g(r)$ against r for the source in water and soft tissue phantoms are shown in figure 6-a. Our results agree well with those of Murphy *et al.* ⁽¹⁰⁾ who measured in virtual water phantom. Maximum percentage of difference was about 5.2%. A third order polynomial fit of the MCNP radial dose function in a water medium has been yielded the following relationship:

$$g(r) = 0.99465 + 0.01161 r - 0.03696 r^2 + 0.00318 r^3$$

The square of correlation coefficient for the polynomial fitting was 0.99778, which was very close to unit as a goodness fitting value.

Also, figure 6-b shows a comparison of $F(1 \text{ cm}, \theta)$ obtained in this study and the results of Murphy *et al.* ⁽¹⁰⁾; which maximum difference is 4% at $\theta=10^\circ$ and the mean difference was less than 1.5% over the all angels. Therefore, the benchmark of computational results with the experimental results seems compatible.

In conclusion, the isodose curves of the ^{131}Cs source model CS-1 have been derived from dose calculation for water and soft tissue phantoms by MCNP code. The result shows dose deposition in high gradient region, near the source, can only be calculated accurately by Monte Carlo method. Results show the PDD is falling in about 5 mm from reference point about 4 times. So, this seed dose not advised to apply in small tumors with size smaller than 5mm. The calculated TG-43 brachytherapy dosimetry parameters for the source agree quite well with Monte Carlo result of Murphy *et al.* ⁽¹⁰⁾ and are useful in treatment in therapeutic plan. The present work demonstrates a useful approach using MCNP code in dose calculation that can be applied in many other fields.

Table 3. Computational value of $F(r, \theta)$ against r at 0° to 80° interval in water and soft tissue phantom.

	θ (deg)	r (cm)										
		0.5	0.75	1	1.5	2	2.5	3	4	5	6	7
In soft tissue phantom	10	---	---	0.719	0.729	0.756	0.769	0.773	0.785	0.796	0.828	0.796
	20	0.792	0.785	0.781	0.808	0.827	0.838	0.847	0.856	0.863	0.864	0.861
	30	0.883	0.879	0.854	0.875	0.889	0.891	0.899	0.902	0.895	0.898	0.899
	40	0.922	0.913	0.908	0.915	0.922	0.923	0.926	0.927	0.928	0.931	0.939
	50	0.951	0.952	0.950	0.954	0.958	0.959	0.962	0.969	0.968	0.967	0.968
	60	0.975	0.976	0.978	0.977	0.979	0.978	0.979	0.977	0.979	0.975	0.979
	70	0.996	0.993	0.993	0.992	0.997	0.988	0.988	0.990	0.988	0.987	0.987
	80	1.001	1.003	1.001	0.998	0.997	0.998	0.997	1.003	0.999	0.998	0.997
In water phantom	10	---	---	0.749	0.765	0.770	0.789	0.801	0.816	0.835	0.869	0.836
	20	0.815	0.816	0.812	0.821	0.831	0.852	0.870	0.872	0.886	0.897	0.901
	30	0.908	0.902	0.903	0.907	0.910	0.912	0.912	0.914	0.917	0.920	0.924
	40	0.938	0.935	0.939	0.936	0.940	0.941	0.944	0.941	0.939	0.937	0.931
	50	0.966	0.961	0.959	0.961	0.962	0.967	0.969	0.966	0.967	0.970	0.958
	60	0.983	0.978	0.976	0.977	0.979	0.983	0.981	0.980	0.982	0.979	0.975
	70	0.991	0.991	0.990	0.991	0.992	0.994	0.989	0.988	0.989	0.990	0.990
	80	0.998	1.001	0.996	0.992	1.001	0.998	0.993	0.997	0.994	1.001	0.987

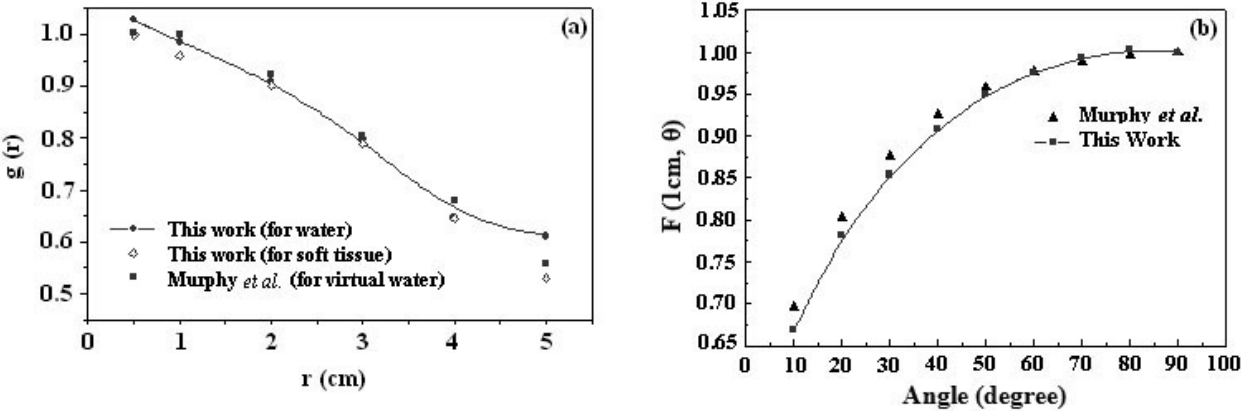


Figure 5. Comparison of the results of this study with the results of Murphy et al. ⁽¹⁰⁾ (a) $g(r)$ value against r ; (b) $F(1\text{ cm}, \theta)$ against θ .

REFERENCES

1. Armpilia CI, Dale RG, Coles IP, Jones B, Antipas V (2003) The determination of radiobiologically, optimized half-lives for radionuclides used in permanent brachytherapy implants. *Int J Radiat Oncol Biol Phys*, **55**: 378-385.
2. Lief E (2005) Modern Advances in Prostate Brachytherapy. *AAPM Brachytherapy School Seattle*.
3. Nath R (2005) Source and Delivery System I: Radionuclides. *AAPM Summer School Yale University*.
4. Nath R, Anderson LL, Luxton G, Weaver KA, Williamson JF, Meigooni AS (1995) Dosimetry of interstitial brachytherapy sources: recommendations of the AAPM Radiation Therapy Committee Task Group No. 43, American Association of Physicists in Medicine. *Med Phys*, **22**: 209-234.
5. Loevinger R (1993) Wide-angle free-air chamber for calibration of low energy brachytherapy sources. *Med Phys*, **20**: 907.
6. Chen Z, Bongiorno P, Nath R (2005) Dose Rate Constant of a Cesium-131 Interstitial Brachytherapy Seed Measured by Thermoluminescent Dosimetry and Gamma-ray Spectroscopy. *Med Phys*, **32**: 3279-85.
7. Williamson JF, Coursey BM, DeWerd LA, Hanson WF, Nath R (1998) Dosimetric prerequisites for routine clinical use of new low energy photon interstitial brachytherapy sources. *Med Phys*, **25**: 2269-2270.
8. Furhang EE, Anderson LL (1998) Functional fitting of interstitial brachytherapy dosimetry data recommended by the AAPM Radiation Therapy Committee Task Group 43. *Med Phys* **26**: 153-160.
9. Henschke UK, Lawrence DC (1965) Cesium-131 seeds for permanent implants. *Radiology* **85**: 1117-1119.
10. Murphy MK, Piper RK, Greenwood LR, Mitch MG, Lamperti PJ, Seltzer SM, Bales MJ, Phillips MH (2004) Evaluation of the new cesium-131 seed for use in low-energy x-ray brachytherapy. *Med Phys*, **31**: 1529-38.
11. The Web site: <http://www.cesium131.com/cesium-history.html>
12. Briesmeister JF (2000) MCNP A general Monte Carlo N-particle transport code, Version 4C, Los Alamos National laboratory Report LA-13709-M, USA.
13. Wittman RS, Fisher DR (2007) Multiple estimate Monte Carlo calculation of the dose rate constant for a cesium-131 interstitial brachytherapy seed. *Med Phys*, **34**: 49-54.
14. Rivard MJ (2001) A discretized approach to determining TG-43 brachytherapy dosimetry parameters: case study using Monte Carlo calculations for the MED3633 103Pd source. *Appl Radiat Iso*, **55**: 775-782.
15. Jarret JM (2005) Experimental method development for permanent interstitial